Bright Side of the Coulomb Blockade

M. Hofheinz, F. Portier, Q. Baudouin, P. Joyez, D. Vion, P. Bertet, P. Roche, and D. Esteve

Service de Physique de l'Etat Condensé (CNRS URA 2464), IRAMIS, CEA Saclay, 91191 Gif-sur-Yvette, France

(Received 28 January 2011; published 27 May 2011)

We explore the photonic (bright) side of the dynamical Coulomb blockade (DCB) by measuring the radiation emitted by a dc voltage-biased Josephson junction embedded in a microwave resonator. In this regime Cooper pair tunneling is inelastic and associated with the transfer of an energy $2eV$ into the resonator modes. We have measured simultaneously the Cooper pair current and the photon emission rate at the resonance frequency of the resonator. Our results show two regimes, in which each tunneling Cooper pair emits either one or two photons into the resonator. The spectral properties of the emitted radiation are accounted for by an extension to DCB theory.

DOI: 10.1103/PhysRevLett.106.217005 PACS numbers: 74.50.+r, 73.23.Hk, 85.25.Cp

The dynamical Coulomb blockade (DCB) of tunneling is a quantum phenomenon in which tunneling of charge through a small tunnel junction is modified by its electromagnetic environment [1–4]. This environment is described as an impedance in series with the tunnel element [see Fig. 1(a)]. The sudden charge transfer associated with tunneling can generate photons in the electromagnetic modes of the environment. In a normal metal tunnel junction, biased at voltage V, the energy eV of a tunneling electron can be dissipated both into quasiparticle excitations in the electrodes and into photons. At low temperature energy conservation forbids tunneling processes emitting photons with total energy higher than eV. This suppression reduces the conductance at low bias voltage [1,2,4]. In a Josephson junction, DCB effects are more prominent since at bias voltages smaller than the gap voltage $2\Delta/e$ quasiparticle excitations cannot take away energy. Therefore, as sketched in Fig. 1(a), the entire energy $2eV$ of tunneling Cooper pairs has to be transformed into photons in the impedance for a dc current to flow through the junction [3,4]. Experiments have confirmed the predictions of DCB theory for the tunneling current, both in the normal [5–7] and superconducting case [8,9] but the associated emission of photons into the environment has never been investigated. The aim of this work is to fill this gap by exploring the photonic side of DCB. We do so by embedding a Josephson junction into a well controlled electromagnetic environment provided by a microwave resonator. The resonator in turn leaks photons into an amplifier, allowing us to measure the rate and spectrum of photons emitted by the junction.

The experimental setup is represented in Fig. 1(b). A small SQUID acts as a tunable Josephson junction with Josephson energy $E_J = E_{J0}|\cos(e\Phi/\hbar)|$ adjustable via the magnetic flux Φ threading its loop. The microwave resonator is made of two quarter-wave transformers and its fundamental mode has frequency $\nu_0 \simeq 6.0$ GHz and quality factor $Q_0 \simeq 9.4$. Higher modes of the resonator appear at $\nu_n \simeq (2n+1)\nu_0$ $(n = 1, 2, \ldots)$ with the same line shape up to small deviations caused by the junction capacitance (estimated to be 4 fF). The expected total impedance $Z(\nu)$ seen by the Josephson element is plotted in the top panels of Figs. 2 and 3, and reaches $\simeq 1.5$ kΩ for all modes.

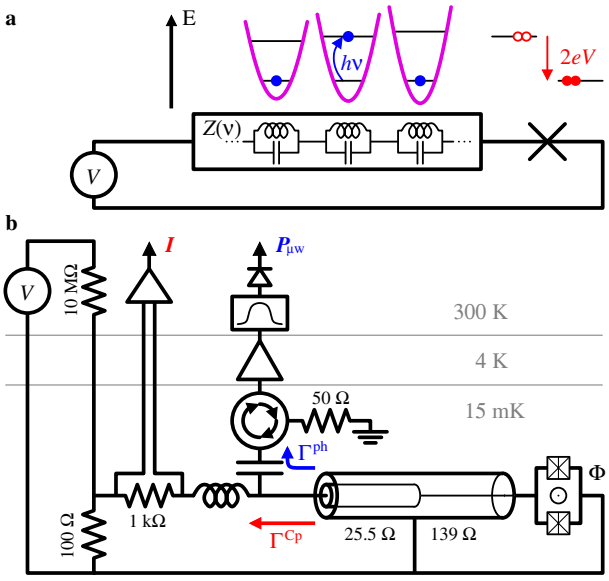

FIG. 1 (color online). The dynamical Coulomb blockade of Josephson tunneling. (a) Generic circuit: a dc voltage-biased Josephson element in series with an electromagnetic environment with impedance $Z(\nu)$, which can be described as a collection of harmonic oscillators. Below the gap voltage, the energy $2eV$ of a tunneling Cooper pair is transferred to the electromagnetic environment in form of one or several photons in its modes. (b) Experimental setup: The sample consists of a SQUID, working as a tunable Josephson junction, in series with a microwave resonator, forming the electromagnetic environment and consisting of two quarter-wave transformers. A bias tee separates the low-frequency voltage bias V and current measurement I from the emitted microwave power $P_{\mu w}$. Three circulators (only one shown) ensure thermalization of the microwave environment. The emitted power is amplified at 4.2 K and then band pass filtered and detected at room temperature.

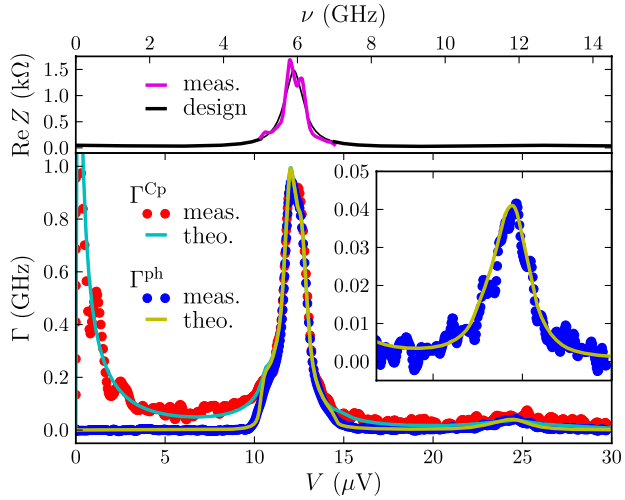

FIG. 2 (color online). Fundamental mode ν_0 of the resonator and corresponding Cooper pair and photon rates. Top panel: real part of the impedance seen by the junction, calculated from the resonator geometry (black line) and reconstructed (magenta) from a quasiparticle shot noise measurement [10]. Bottom panel: measured Cooper pair rate Γ^{Cp} (red) and photon rate Γ_0^{ph} (blue) integrated from 5 to 7 GHz. Both rates show a peak around $V = h\nu_0/2e \simeq 12\ \mu$V. A second small peak in the microwave power at $V = 24\ \mu$V (vertical zoom in inset) corresponds to two-photon processes. Solid lines are $P(E)$ theory fits using the reconstructed impedance from 5 to 7 GHz and the calculated impedance elsewhere, an effective temperature of 60 mK, and a single adjustable parameter $E_J = 5.1\ \mu$eV. Cyan and yellow lines correspond, respectively, to Eq. (1) and (5) integrated from 5 to 7 GHz.

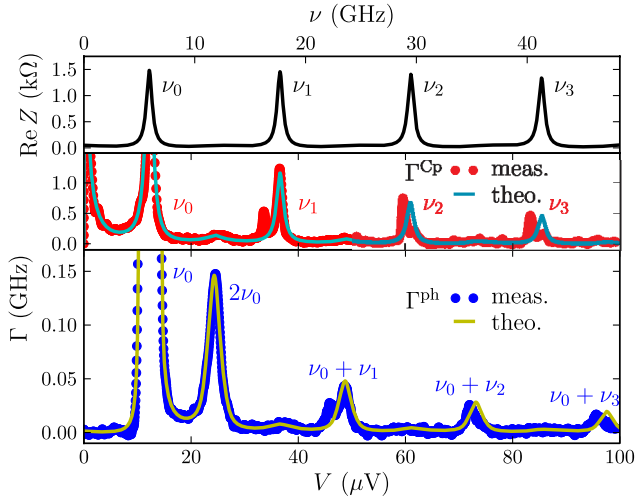

FIG. 3 (color online). Harmonics ν_n of the resonator and corresponding Cooper pair and photon rates. The plotted quantities are the same as in Fig. 2, but for a larger voltage and frequency range and different Josephson coupling. The Cooper pair rate shows peaks at voltages $V = h\nu_n/2e$, associated with the emission of photons in the resonator mode at frequency ν_n. The power measurement only probes the photons emitted in the fundamental mode of the resonator. It shows a large peak at $V = h\nu_0/2e$, and smaller ones at $V = h(\nu_0 + \nu_n)/2e$, due to simultaneous emission of one photon at ν_0 and one photon at ν_n per tunneling Cooper pair. Here theoretical curves are obtained from the calculated impedance and the fitting parameter $E_J = 10.3\ \mu$eV.

The sample is cooled to $T \simeq 15$ mK in a dilution refrigerator and connected to a bias tee separating the high-frequency and low-frequency components of the current. The low-frequency port is connected to a voltage bias through a 1 kΩ resistor used to measure the tunneling current I. The high-frequency port is connected to a 4 to 8 GHz cryogenic amplifier with noise temperature $T_N \simeq 3.5$ K through three circulators protecting the sample from the amplifier noise and ensuring thermalization of the environment. After further amplification and band pass filtering at room temperature, the power is detected using a calibrated square-law detector. Its output voltage is proportional to the microwave power, which contains the weak sample contribution $P_{\mu w}$ on top of the large noise floor of the cryogenic amplifier. In order to remove this background we bias the sample with a low frequency 0 to V square-wave modulation and perform a lock-in detection of the induced square-wave response of the detector.

We first characterize the on-chip microwave resonator and determine the gain of the microwave chain by measuring the power emitted by the electronic shot noise of the junction $S_{II} \simeq eI$ at bias voltage $V \simeq 2$ mV, well above the gap voltage $2\Delta/e \simeq 0.4$ mV. Under these conditions, the spectral density of the emitted power is $2eV\mathrm{Re}Z(\nu)R_N/|R_N + Z(\nu)|^2 \simeq 2eV\mathrm{Re}Z(\nu)/R_N$ with $R_N = 17.9\ \mathrm{k}\Omega \gg |Z(\nu)|$ the tunnel resistance of the junction in the normal state. This spectral density is extracted using a heterodyne measurement equivalent to a 100 MHz wide band pass at tunable frequency. More details about this procedure can be found in [10]. The extracted $\mathrm{Re}Z(\nu)$ is shown in the upper panel of Fig. 2 and the right panel of Fig. 4. It shows the expected peak at ν_0 with an additional modulation due to parasitic reflections in the microwave setup.

Once the system calibrated, we measure the Cooper pair transfer rate across the SQUID $\Gamma^{\mathrm{Cp}} = I/2e$ and the photon emission rate into the fundamental mode of the resonator Γ_0^{ph} as a function of bias voltage. Rate Γ_0^{ph} is extracted from the microwave power $P_{\mu w}$, emitted in a 2 GHz wide band centered at $\nu_0 = 6$ GHz, via $\Gamma_0^{\mathrm{ph}} = P_{\mu w}/h\nu_0$. In order to simplify interpretation of our data, we adjust E_J for each experiment to ensure good signal to noise ratio while keeping the maximum Γ_0^{ph} smaller than the decay rate of the resonator $2\pi\nu_0/Q_0 \simeq 4$ GHz, so that the electromagnetic environment of the junction stays close to thermal equilibrium.

The measured rates Γ^{Cp} and Γ_0^{ph} are shown in Figs. 2 and 3. In Fig. 2 both rates display a peak at voltage $V_0 = h\nu_0/2e = 12\ \mu$V, where the energy of a tunneling

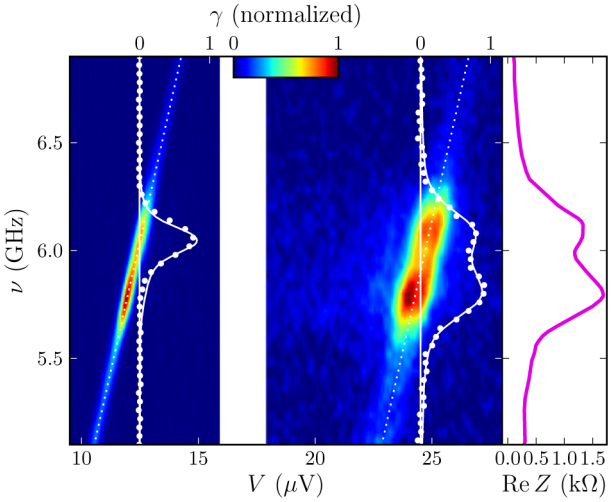

FIG. 4 (color online). Main panel: spectral density of the photon emission rate γ for the first and second order peaks (ν_0 and $2\nu_0$) as a function of bias voltage and frequency. Data were taken for different Josephson energies and were normalized by the maximum γ of each data set. Dotted lines correspond to $2eV = h\nu$ and $2eV = h(\nu + \nu_0)$. White dots correspond to power spectra at fixed voltages (12.5 and 24.5 μeV) and solid lines to theoretical predictions Eq. (5) integrated over 100 MHz, the width of the filter used in this experiment, with effective temperature 60 mK and fitting parameters $E_J = 5.0$ μeV at $V = 12.5$ μV and $E_J = 14.3$ μeV at $V = 24.5$ μV. Right panel: reconstructed dissipative part of the resonator impedance, as in Fig. 2.

Cooper pair corresponds to the energy of one photon at frequency ν_0. On resonance Γ^{Cp} and Γ_0^{ph} agree within 5%. In Fig. 3 additional peaks appear in Γ^{Cp} at voltages $V_n = h\nu_n/2e$ ($n = 1, 2, 3$), which do not have counterparts in Γ_0^{ph}. In both figures Γ^{Cp} and Γ_0^{ph} show much smaller peaks at $V_0 + V_n$ ($n = 0, 1, 2, 3$).

DCB theory accounts for these results. At low temperature $k_BT \ll 2eV$, when backward tunneling is negligible, the Cooper pair rate is given by [3,4]

$$\Gamma^{\mathrm{Cp}} = \frac{\pi}{2\hbar} E_J^2 P(2eV), \tag{1}$$

where $P(E)$ is the probability density for a tunneling charge $2e$ to emit energy E in form of photons into the impedance. The function $P(E)$ is the Fourier transform of $\exp J(t)$ with [4]

$$J(t) = 2\int_{-\infty}^{\infty} d\nu \frac{r(\nu)}{\nu} \frac{\exp(-i2\pi\nu t) - 1}{1 - \exp(-h\nu/k_BT)}, \tag{2}$$

where

$$r(\nu) = \frac{4e^2}{h} \mathrm{Re}Z(\nu). \tag{3}$$

At $T = 0$, the expansion of $P(E)$ in powers of $r(\nu)$ yields

$$\Gamma^{\mathrm{Cp}} \simeq \frac{E_J^{*2}}{2\hbar^2}\left(\frac{r(\nu_J)}{\nu_J} + \int_0^{\nu_J} d\nu \frac{r(\nu)}{\nu} \frac{r(\nu_J - \nu)}{\nu_J - \nu}\right), \tag{4}$$

where $E_J^* = E_J(1 - \int d\nu r(\nu)/\nu)$ and $\nu_J = 2eV/h$. We neglect here the low-frequency environment and suppose $\int d\nu r(\nu)/\nu \ll 1$. The first term in the parenthesis of Eq. (4) corresponds to the emission of a single photon at frequency ν_J. It accounts for the peaks in Γ^{Cp} observed at bias voltages V_n and for the peak in Γ_0^{ph} at V_0. Since we only detect photons emitted in the fundamental mode, Γ_0^{ph} does not show any peak at V_n for $n > 0$. The second term in the parenthesis corresponds to the simultaneous emission of two photons at frequencies ν and $\nu_J - \nu$. It accounts for the peaks in Γ_0^{ph} observed at bias voltages $V_0 + V_n$, where the energy of a tunneling Cooper pair can be split into one photon at frequency ν_0 and another at frequency ν_n. These two-photon processes have much lower rates than the single photon processes because of the low resonator impedance. They also contribute to the peaks in Γ^{Cp} between the main resonances. Note, however, that, due to a small rise in $\mathrm{Re}Z(\nu)$ at $\nu_0 + \nu_n$, single photon processes contribute about equally to the peaks in Γ^{Cp} at bias voltages $V_0 + V_n$. Equation (4) also accounts for the increase in Γ^{Cp} at low voltage in Fig. 2 and the reduction of the height of the resonances at V_n with increasing n, which both reflect the $1/\nu$ scaling of the first-order term. Note that as far as single photon processes are concerned, the ac Josephson effect predicts the same voltage to frequency conversion and Cooper pair and photon rates. However, DCB assumes that the transferred charge is almost a classical variable and its conjugate variable, the phase across the junction, has large quantum fluctuations, whereas the opposite assumption is made in the ac Josephson effect.

In Fig. 4 we explore the spectral properties of the emitted radiation using a heterodyne technique with 100 MHz resolution. The first-order emission occurs along a narrow line at $2eV = h\nu$ whose amplitude is modulated by $r(\nu)$, in agreement with Eq. (4). This equation, however, makes no prediction about the spectral width of the emitted radiation which is found to be approximately 150 MHz, significantly narrower than the 700 MHz wide resonance in $r(\nu)$. The second order peak follows a $2eV = h(\nu + \nu_0)$ line and has a much broader spectral width, comparable to the width of the resonance in $r(\nu)$.

In order to account for these observations we calculate the spectral density of the photon emission rate $\gamma(\nu)$ in the DCB regime, which is related to the emission current noise spectral density S_{II} via $\gamma = 2\mathrm{Re}Z(\nu)S_{II}(\nu)/h\nu$. $\gamma(\nu)$ is the average population of the outgoing photon modes. From the relation between S_{II} and $P(E)$ [3,10] one obtains

$$\gamma = \frac{2r(\nu)}{\nu} \frac{\pi}{2\hbar} E_J^2 P(2eV - h\nu). \tag{5}$$

This expression, valid at low temperature $k_BT \ll h\nu$, $2eV$, can be understood within a Caldeira-Leggett

decomposition [11] of the impedance $Z(\nu)$ into modes with infinitesimal width [10]: The term $2r(\nu)/\nu$ describes the probability density for each tunneling Cooper pair to emit a photon at frequency ν into the environment. The remainder of Eq. (5) gives the Cooper pair rate while emitting the remaining energy $2eV - h\nu$ in the form of one or several other photons, as in Eq. (1).

The first-order peak occurs at $2eV \simeq h\nu$, so that $P(E)$ has to be evaluated around $E \simeq 0$ where the perturbative expression (4) is not valid. Therefore we calculate $P(E)$ at all orders in r at finite temperature, following the method described in Ref. [12]. $P(E \simeq 0)$ is approximately a Lorentzian $\frac{D/\pi}{D^2+E^2}$ of width $2D \simeq 4\pi k_B T r(0)$ [12]. This expression gives the spectral width of the first-order peak. Its height along the line $2eV = h\nu$ follows the variations of $r(\nu)$ due to the first term in Eq. (5). In order to find a quantitative agreement with the data we use an effective temperature $T = 60$ mK, in good agreement with the 60 mK $\pm$ 10 mK electronic temperature deduced from shot noise measurements performed at ν_0 on the same junction, driven to the normal state by applying a 0.1 T magnetic field [13]. We attribute the difference between the effective temperature of the environment and the fridge temperature of 15 mK mainly to low-frequency noise radiated by the amplifier used for the current measurement.

For the second order peak $P(E)$ has to be evaluated around $E \simeq h\nu_0$, where it reproduces the variations of $r(E/h)$. The radiation of the second order peak is therefore emitted in a band around $2eV = h(\nu_0 + \nu)$ with a spectral width given by the width of the resonance in $r(\nu)$. As for the first-order peak, the amplitude along this line is then modulated by $r(\nu)$ due to the first term in Eq. (5).

With the spectral distribution γ at hand we now come back to the data presented in Figs. 2 and 3 for a more quantitative description. The solid yellow lines in both figures show expression (5), integrated from 5 to 7 GHz, and the solid cyan lines expression (1) [14]. The theory accurately matches the measurement with a single fitting parameter, the Josephson energy E_J, and accounts for the relative weight of the first and second order peaks in Fig. 2. Discrepancies only show up at the larger bias voltages in Fig. 3, corresponding to frequencies above 18 GHz where we do not accurately control the electromagnetic environment. For the sake of consistency with Fig. 4 we have used the non perturbative $P(E)$, although the zero temperature perturbative expression (4) would already have given a satisfactory agreement with the data.

In conclusion, our results clearly validate the understanding of DCB based on photon emission into the electromagnetic environment. We have measured the spectral density of the emitted radiation, which we quantitatively account for by an extension to DCB theory. A natural continuation of this work is the investigation of tunneling current and emitted radiation at higher Josephson energy, where the emission rate can be strong enough to overcome cavity loss and cause stimulated emission. A larger Josephson energy will also make simultaneous tunneling of multiple Cooper pairs relevant. These are the two ingredients for the transition from the DCB regime to the regime of the ac Josephson effect. Furthermore, our results demonstrate that under appropriate biasing, the tunneling of a Cooper pair is associated with the simultaneous emission of multiple photons. This opens the way to new schemes for the emerging field of microwave quantum optics with itinerant photons [15–17].

We gratefully acknowledge support from the European project Scope, the ANR project Masquelspec, C'Nano IdF, technical help from P. Senat, P. Jacques, P. Orfila, and discussions with M. Devoret and within the Quantronics group.

[1] M. H. Devoret *et al.*, Phys. Rev. Lett. **64**, 1824 (1990).
[2] S. M. Girvin *et al.*, Phys. Rev. Lett. **64**, 3183 (1990).
[3] D. Averin, Y. Nazarov, and A. Odintsov, Physica (Amsterdam) **165–166B**, 945 (1990).
[4] G.-L. Ingold and Y. V. Nazarov, in *Single Charge Tunneling*, edited by H. Grabert and M. H. Devoret (Plenum, New York, 1992).
[5] P. Delsing *et al.*, Phys. Rev. Lett. **63**, 1180 (1989).
[6] L. J. Geerligs *et al.*, Europhys. Lett. **10**, 79 (1989).
[7] A. N. Cleland, J. M. Schmidt, and J. Clarke, Phys. Rev. Lett. **64**, 1565 (1990).
[8] T. Holst *et al.*, Phys. Rev. Lett. **73**, 3455 (1994).
[9] J. Basset, H. Bouchiat and R. Deblock, Phys. Rev. Lett. **105**, 166801 (2010).
[10] See supplemental material at http://link.aps.org/supplemental/10.1103/PhysRevLett.106.217005.
[11] A. Caldeira and A. Leggett, Ann. Phys. (N.Y.) **149**, 374 (1983).
[12] G.-L. Ingold and H. Grabert, Europhys. Lett. **14**, 371 (1991).
[13] R. J. Schoelkopf *et al.*, Phys. Rev. Lett. **78**, 3370 (1997).
[14] The theory line corresponds actually to $\frac{\pi}{2\hbar}E_J^2(P(2eV) - P(-2eV))$, but the backward tunneling term is unimportant above approximately 1 μV
[15] A. A. Houck *et al.*, Nature (London) **449**, 328 (2007).
[16] D. Bozyigit *et al.*, Nature Phys. **7**, 154 (2010).
[17] F. Mallet *et al.*, arXiv:1012.0007v1 [Phys. Rev. Lett. (to be published)].